

## Research Article

Azzh Saad Alshehry, Humaira Yasmin\*, Abdul Hamid Ganie, Muhammad Wakeel Ahmad, and Rasool Shah

# Optimal auxiliary function method for analyzing nonlinear system of coupled Schrödinger–KdV equation with Caputo operator

<https://doi.org/10.1515/phys-2023-0127>  
received July 29, 2023; accepted October 07, 2023

**Abstract:** The optimal auxiliary function method (OAFM) is introduced and used in the analysis of a nonlinear system containing coupled Schrödinger–KdV equations, all within the framework of the Caputo operator. The OAFM, known for its efficiency in solving nonlinear issues, is used to obtain approximate solutions for the coupled equations' complicated dynamics. Numerical and graphical assessments prove the suggested method's correctness and efficiency. This study contributes to the understanding and analysis of coupled Schrödinger–KdV equations and their many applications by providing insights into the behavior of nonlinear systems within mathematical physics.

**Keywords:** optimal auxiliary function method, nonlinear system of Schrödinger–KdV equation, Caputo operator, fractional calculus

## 1 Introduction

Fractional partial differential equations (FPDEs) have arisen as a strong mathematical framework for explaining complex systems that show anomalous diffusion, memory

effects, and nonlocal interactions. These equations incorporate fractional-order derivatives derived within the context of fractional calculus and so generalize traditional partial differential equations [1–5]. Due to their capacity to simulate complex dynamics that conventional integer-order derivatives cannot fully represent, FPDEs are used in many scientific fields, including biology, engineering, and finance [6–8]. It is possible to trace the theoretical roots of fractional calculus to the pioneering work of mathematicians like Riemann, Liouville, and Caputo [9–11]. However, the promise of FPDEs to provide more precise and realistic representations of diverse natural and artificial systems has only recently attracted substantial attention [12–14]. This introduction's goal is to give a general understanding of fractional calculus's core ideas and how they apply to FPDEs while also identifying important sources that have shaped this field's development [14–18].

The study of nonlinear systems has revealed complex dynamics crucial to several scientific fields. A notable area of study among them is the coupling of the Schrödinger and Korteweg–de Vries (KdV) equations. These equations are important tools for understanding a wide range of physical events because they capture key aspects of wave propagation and soliton processes. The combination of the nonlinear dispersive KdV equation with the quantum mechanical Schrödinger equation results in a coupled system that exhibits intricate interactions between linear and nonlinear processes [19–21]. In addition to offering a more comprehensive framework for comprehending wave dynamics, this coupling also creates opportunities for investigating fascinating phenomena that result from their interdependence. To acquire an understanding of the interaction between quantum and nonlinear dynamics and its larger ramifications across scientific fields, this work investigates the analysis of the nonlinear system of coupled Schrödinger–KdV equations in all of its complexity [22–24].

Understanding the complex behavior of many physical events requires understanding nonlinear systems, which offers an enthralling panorama. The investigation

\* **Corresponding author: Humaira Yasmin**, Department of Basic Sciences, Preparatory Year Deanship, King Faisal University, Al-Ahsa, 31982, Saudi Arabia, e-mail: hhasain@kfu.edu.sa

**Azzh Saad Alshehry:** Department of Mathematical Sciences, Faculty of Sciences, Princess Nourah Bint Abdulrahman University, P.O. Box 84428, Riyadh 11671, Saudi Arabia, e-mail: asalshihry@pnu.edu.sa

**Abdul Hamid Ganie:** Basic Science Department, College of Science and Theoretical Studies, Saudi Electronic University, Riyadh 11673, Saudi Arabia, e-mail: a.ganie@seu.edu.sa

**Muhammad Wakeel Ahmad:** Department of Mathematics, Abdul Wali Khan University Mardan, Mardan, Pakistan, e-mail: wakee.math@gmail.com

**Rasool Shah:** Department of Mathematics, Abdul Wali Khan University Mardan, Mardan, Pakistan, e-mail: shahrasool26@gmail.com

of coupled Schrödinger–KdV equations is one especially fascinating direction in this area. The Schrödinger equation, which regulates the behavior of wave functions in quantum mechanics, and the Korteweg–de Vries equation, which is well known for its role in explaining nonlinear wave propagation and soliton production, are combined in these equations. A new system that captures both linear quantum effects and nonlinear dispersive dynamics is created by linking these equations, offering a singular opportunity to investigate the interactions between these several physical phenomena [25].

In addition to enhancing our knowledge of wave processes, this coupling also has potential applications in several other disciplines, including fluid dynamics and nonlinear optics [26–28]. Understanding the deep links between quantum effects and nonlinear interactions would help researchers understand the complex mechanisms that influence wave behavior in challenging physical contexts [29–31]. This work attempts to reveal the basic insights that result from the coupling of the nonlinear system of coupled Schrödinger–KdV equations, providing a greater understanding of the complicated dynamics and interdependencies that underpin complex wave propagation situations [32,33]. We want to contribute to the better knowledge of nonlinear systems and their importance in various scientific areas via thorough analysis and numerical research [34–36].

The search for efficient methods for resolving nonlinear equations and systems has taken center stage in many scientific fields. The optimal auxiliary function method (OAFM) has emerged as a potential strategy to solve these issues by providing a structured and adaptable framework. The OAFM, which has its roots in mathematical analysis, aims to approximate solutions by carefully including auxiliary functions that improve convergence characteristics. The method's applicability to various nonlinear situations gives it versatility and makes it useful in disciplines including physics, engineering, and applied mathematics. Using examples from various situations, we examine the theoretical underpinnings, benefits, and practical application of the OAFM in this study [37–39].

Due to its potential for solving challenging nonlinear issues, the OAFM has attracted much interest lately. The OAFM provides a systematic framework for approximation solutions that could otherwise be difficult to acquire by efficiently integrating components of perturbation theory, auxiliary functions, and optimization approaches. The OAFM was used by Lu et al. [40] to tackle nonlinear computational intelligence systems, demonstrating its capacity to extract multiscale characteristics from mixed picture and text input. In the study of Yin et al. [41], a novel end-to-end lake boundary prediction model. This demonstrates

how the approach may be used in various fields and highlights its promise as a tool for studying challenging real-world circumstances.

Furthermore, Chen et al. [42], who used the technique to create a generic linear free-energy relationship for forecasting partition coefficients in organic compounds, highlighted the OAFM's potency in handling mathematical models. This application highlights the OAFM's ability to draw important correlations from complex mathematical formulations. Furthermore, Lu et al. [43] discussed attention processes in the context of multi-modal fusion in visual question responding, emphasizing how the OAFM might illuminate the intricate interaction of diverse data sources.

The OAFM has shown promise in various applications, from feature extraction to predictive modeling. To contribute to the expanding body of knowledge on efficient nonlinear problem-solving strategies, this work clarifies the method's theoretical foundations, investigates its benefits, and offers insights into its practical application.

## 2 Preliminaries

**Definition.** The fractional Caputo derivative of a function  $U(\zeta, \tau)$  of order  $\alpha$  is given as follows:

$${}^C D_t^\alpha U(\zeta, t) = J_t^{m-\alpha} U^m(\zeta, t), \quad m-1 < \alpha \leq m, \quad t > 0. \quad (1)$$

**Definition.** The formula for the Riemann fractional integral is as follows:

$$J_t^\alpha U(\zeta, t) = \frac{1}{\Gamma(\alpha)} \int_0^t (t-r)^{\alpha-1} U(\zeta, r) dr \quad (2)$$

**Lemma.** For  $n-1 < \alpha \leq n$ ,  $p > -1$ ,  $t \geq 0$ , and  $\lambda \in \mathbb{R}$ , we have:

1.  $D_t^\alpha t^p = \frac{\Gamma(\alpha+1)}{\Gamma(p-\alpha+1)} t^{p-\alpha}$
2.  $D_t^\alpha \lambda = 0$
3.  $D_t^\alpha I_t^\alpha U(\zeta, t) = U(\zeta, t)$
4.  $I_t^\alpha D_t^\alpha U(\zeta, t) = U(\alpha, t) - \sum_{i=0}^{n-1} \partial^i U(\zeta, 0) \frac{t^i}{i!}$

## 3 General procedure of OAFM

To elucidate the fundamental concept of the OAFM, we shall dissect a general nonlinear equation represented as follows:

$$L(u) + N(u) + h(\varphi) = 0. \quad (3)$$

This equation is accompanied by the given initial/boundary conditions:

$$B(u(\varphi), \frac{\partial u(\varphi)}{\partial \varphi}) = 0. \quad (4)$$

In this context,  $L$  pertains to the linear term,  $N$  denotes the nonlinear term, and  $h$  is a given function. The approach involves the approximation of the solution for Eq. (3), which can be expressed as follows:

$$u^*(\varphi, C_i) = u_0(\varphi) + u_1(\varphi, C_n), \quad n = 1, 2, 3, 4 \dots s. \quad (5)$$

To initiate this approximation process, we derive the initial and first approximations for Eq. (3) by introducing Eq. (5) into Eq. (3), yielding

$$L(u_0(\varphi) + u_1(\varphi, C_n)) + N(u_0(\varphi) + u_1(\varphi, C_n)) + h(\varphi) = 0. \quad (6)$$

The initial approximation, denoted as  $u_0(\varphi)$ , can be obtained from the linear term, leading to

$$L(u_0(\varphi)) + h(\varphi) = 0, \quad B\left(u_0, \frac{du_0}{d\varphi}\right) = 0. \quad (7)$$

The linear operator  $L$  relies on the given initial/boundary conditions, while the function  $h(\varphi)$  remains variable.

To determine the first approximation  $u_1(\varphi)$ , we take into account both the initial approximation and the nonlinear differential equation, along with the corresponding initial/boundary conditions, which results in:

$$L(u_1(\varphi, C_n)) + N(u_0(\varphi) + u_1(\varphi, C_n)) = 0, \quad (8)$$

accompanied by the following relevant initial/boundary conditions:

$$B\left(u_1(\varphi, C_n), \frac{\partial u_1(\varphi, C_n)}{\partial \varphi}\right) = 0. \quad (9)$$

Furthermore, the nonlinear term in Eq. (8) can be expanded as follows:

$$N(u_0 + u_1) = N(u_0) + \sum_{k=1}^{\infty} \frac{u_1^{(k)}}{k!} N^{(k)}(u_0(\varphi)). \quad (10)$$

This expansion, as delineated in Eq. (10), can be presented algorithmically to achieve the limiting solution.

In order to overcome the challenges associated with solving the nonlinear differential equation presented in Eq. (6) and expedite the convergence of the first approximation  $u_1(\varphi, C_n)$ , an alternate expression, as represented in Eq. (7), is introduced for Eq. (8). This expression is vital for controlling the issues encountered during the solution of nonlinear differential equations and enhancing the convergence of the first approximation.

**Remark 1.**  $A_1$  and  $A_2$  are considered auxiliary functions that are contingent on  $u_0(\varphi)$  and unknown parameters  $C_n$  and  $C_m$ , where  $n = 1, 2, 3, \dots s$  and  $m = s + 1, s + 2, s + 3 \dots q$ .

**Remark 2.**  $A_1$  and  $A_2$  are not fixed and may encompass  $u_0(\varphi)$  or  $N(u_0(\varphi))$ , or even a combination of both, depending on the specific context.

**Remark 3.** The nature of  $A_1$  and  $A_2$  depends on whether  $u_0(\varphi)$  or  $N(u_0(\varphi))$  is a polynomial, trigonometric, or exponential function, resulting in corresponding summation forms. In the special case where  $N(u_0(\varphi)) = 0$  and  $u_0(\varphi)$  serves as the exact solution.

**Remark 4.** The determination of the values for the unknown parameters  $C_n$  and  $C_m$  can be achieved using various methods, such as the Ritz method, Collocation method, Least Square method, or Galerkin's method.

This comprehensive approach underlines the flexibility and adaptability of the OAFM in handling a wide range of nonlinear problems.

### 3.1 Problem 1

#### 3.1.1 Implementation of OAFM

Consider the coupled Schrödinger–KdV equation of fractional order

$$D_t^\mu u(\varphi, t) - \partial_{\varphi\varphi} v(\varphi, t) - v(\varphi, t)w(\varphi, t) = 0,$$

where  $0 < \mu \leq 1$

$$D_t^\mu v(\varphi, t) + \partial_{\varphi\varphi} u(\varphi, t) + u(\varphi, t)w(\varphi, t) = 0 \quad (11)$$

$$D_t^\mu w(\varphi, t) + 6w(\varphi, t)\partial_{\varphi} w(\varphi, t) + \partial_{\varphi\varphi\varphi} w(\varphi, t) - 2u(\varphi, t)\partial_{\varphi} u(\varphi, t) - 2v(\varphi, t)\partial_{\varphi} v(\varphi, t) = 0$$

subject to the following initial conditions:

$$\begin{aligned} u(\varphi, 0) &= \tanh(\varphi) \cos(\varphi), \\ v(\varphi, 0) &= \tanh(\varphi) \sin(\varphi), \\ w(\varphi, 0) &= \frac{7}{8} - 2 \tanh^2(\varphi). \end{aligned} \quad (12)$$

Consider the following linear terms from Eq. (11):

$$\begin{aligned} L(u(\varphi, t)) &= D_t^\mu u(\varphi, t), \\ L(v(\varphi, t)) &= D_t^\mu v(\varphi, t), \\ L(w(\varphi, t)) &= D_t^\mu w(\varphi, t). \end{aligned} \quad (13)$$

The nonlinear terms can be defined as:

$$\begin{aligned} N(u(\varphi, t)) &= -\partial_{\varphi\varphi}v(\varphi, t) - v(\varphi, t)w(\varphi, t) \\ N(v(\varphi, t)) &= \partial_{\varphi\varphi}u(\varphi, t) + u(\varphi, t)w(\varphi, t) \\ N(w(\varphi, t)) &= 6w(\varphi, t)\partial_{\varphi}w(\varphi, t) + \partial_{\varphi\varphi\varphi}w(\varphi, t) \\ &\quad - 2u(\varphi, t)\partial_{\varphi}u(\varphi, t) - 2v(\varphi, t)\partial_{\varphi}v(\varphi, t) \end{aligned} \quad (14)$$

Zeroth order approximation

$$\begin{aligned} D_t^\mu u_0(\varphi, t) &= 0, \quad f_0(\varphi, 0) = \tanh(\varphi) \cos(\varphi) \\ D_t^\mu v_0(\varphi, t) &= 0, \quad g_0(\varphi, 0) = \tanh(\varphi) \sin(\varphi) \\ D_t^\mu w_0(\varphi, t) &= 0, \quad h_0(\zeta, 0) = \frac{7}{8} - 2 \tanh^2(\varphi). \end{aligned} \quad (15)$$

Using the inverse operator, we obtain the following solution:

$$\begin{aligned} u_0(\varphi, t) &= \tanh(\varphi) \cos(\varphi) \\ v_0(\varphi, t) &= \tanh(\varphi) \sin(\varphi) \\ w_0(\varphi, t) &= \frac{7}{8} - 2 \tanh^2(\varphi). \end{aligned} \quad (16)$$

Using Eq. (16) in Eq. (14), the system of nonlinear term becomes

$$\begin{aligned} N[u_0(\zeta, t)] &= \frac{17}{8} \sin(\varphi) \tanh(\varphi) - 2 \cos(\varphi) \operatorname{sech}^2(\varphi) \\ N[v_0(\zeta, t)] &= -\frac{17}{8} \cos(\varphi) \tanh(\varphi) - 2 \sin(\varphi) \operatorname{sech}^2(\varphi) \\ N[w_0(\zeta, t)] &= 9 \tanh(\varphi) \operatorname{sech}^2(\varphi), \end{aligned} \quad (17)$$

and we choose the auxiliary function  $A_1, A_2$ , and  $A_3$  as follows:

$$\begin{aligned} A_1 &= c1 \cos(\varphi) \tanh(\varphi) + c2 \cos^3(\varphi) \tanh^3(\varphi), \\ A_2 &= c3 \sin^4(\varphi) \tanh^4(\varphi) + c4 \sin^5(\varphi) \tanh^5(\varphi), \\ A_3 &= c5 \left( \frac{7}{8} - 2 \tanh^2(\varphi) \right)^6 + c6 \left( \frac{7}{8} - 2 \tanh^2(\varphi) \right)^7. \end{aligned} \quad (18)$$

The first-order approximation according to OAFM procedure is discussed in Section 3, i.e.,

$$\begin{aligned} \frac{\partial^\mu u_1(\varphi, t)}{\partial t^\mu} &= -(A_1 N[u_0(\varphi, t)]) \\ \frac{\partial^\mu v_1(\varphi, t)}{\partial t^\mu} &= -(A_2 N[v_0(\varphi, t)]) \\ \frac{\partial^\mu w_1(\varphi, t)}{\partial t^\mu} &= -(A_3 N[w_0(\varphi, t)]). \end{aligned} \quad (19)$$

Using Eqs. (17) and (18) in Eq. (19), we obtain

$$\begin{aligned} \frac{\partial^\mu u_1(\varphi, t)}{\partial t^\mu} &= -\left( (c1 \cos(\varphi) \tanh(\varphi) + c2 \cos^3(\varphi) \tanh^3(\varphi)) \right. \\ &\quad \times \left[ \frac{17}{8} \sin(\varphi) \tanh(\varphi) - 2 \cos(\varphi) \operatorname{sech}^2(\varphi) \right] \Bigg) \\ \frac{\partial^\mu v_1(\varphi, t)}{\partial t^\mu} &= -\left( (c3 \sin^4(\varphi) \tanh^4(\varphi) + c4 \sin^5(\varphi) \tanh^5(\varphi)) \right. \\ &\quad \times \left[ -\frac{17}{8} \cos(\varphi) \tanh(\varphi) - 2 \sin(\varphi) \operatorname{sech}^2(\varphi) \right] \Bigg) \\ \frac{\partial^\mu w_1(\varphi, t)}{\partial t^\mu} &= -9 \tanh(\varphi) \operatorname{sech}^2(\varphi) \\ &\quad \times \left[ c5 \left( \frac{7}{8} - 2 \tanh^2(\varphi) \right)^6 + c6 \left( \frac{7}{8} - 2 \tanh^2(\varphi) \right)^7 \right], \end{aligned} \quad (20)$$

by applying inverse operator to Eq. (20), we obtain

**Table 1:** Absolute error of  $u(\varphi, t)$  at fractional orders  $\mu = 0.7, \mu = 0.8$ , and  $\mu = 1$

$\zeta$	Absolute error <sub>(<math>\mu=0.7</math>)</sub>	Absolute error <sub>(<math>\mu=0.8</math>)</sub>	Absolute error <sub>(<math>\mu=1</math>)</sub>
0.	0.00004	0.00004	0.00004
0.1	0.00130227	0.000404499	0.000004655
0.2	0.00217469	0.000694956	0.0000421961
0.3	0.00236032	0.000759476	0.000053294
0.4	0.00197233	0.000635256	0.0000454302
0.5	0.0013183	0.000423718	0.0000290893
0.6	0.000679637	0.000217624	0.0000138151
0.7	0.000167597	0.0000534943	0.0000036002
0.8	0.00027163	0.0000866903	0.00000510754
0.9	0.00074588	0.000238765	0.00001506
1.	0.0012967	0.000416593	0.0000283522

**Table 2:** Absolute error of  $v(\varphi, t)$  at fractional orders  $\mu = 0.55, \mu = 0.75$ , and  $\mu = 1$

$\zeta$	Absolute error <sub>(<math>\mu=0.55</math>)</sub>	Absolute error <sub>(<math>\mu=0.75</math>)</sub>	Absolute error <sub>(<math>\mu=1</math>)</sub>
0.5	0.000577801	0.0000354637	0.0000281522
0.6	0.00191544	0.000181767	0.0000215926
0.7	0.0043588	0.000452243	0.00000599374807
0.8	0.00732438	0.000781972	0.0000145519
0.9	0.00921167	0.000992997	0.0000289521
1.	0.00812713	0.000874782	0.0000240854
1.1	0.00317805	0.00032797	0.0000006343112
1.2	0.0045951	0.000532017	0.0000554198
1.3	0.0123911	0.00139412	0.000104191
1.4	0.0169013	0.00189093	0.000130217
1.5	0.0159235	0.00177787	0.00011859

**Table 3:** Absolute error of  $w(\varphi, t)$  at fractional orders  $\mu = 0.6$ ,  $\mu = 0.8$ , and  $\mu = 1$

$\zeta$	Absolute error <sub>(<math>\mu=0.6</math>)</sub>	Absolute error <sub>(<math>\mu=0.8</math>)</sub>	Absolute error <sub>(<math>\mu=1</math>)</sub>
1.3	0.000530974	0.0000269316	0.0000288141
1.37	0.000887848	0.0000693315	0.0000211942
1.44	0.00131683	0.000119502	0.0000129191
1.51	0.00178548	0.000173845	0.00000439
1.58	0.00225593	0.000228179	0.00000391539
1.65	0.00269217	0.000278529	0.000011588
1.72	0.00306528	0.000321714	0.0000182843
1.79	0.00335612	0.000355633	0.0000237875
1.86	0.00355569	0.000379302	0.0000280033
1.93	0.00366383	0.00039272	0.0000309441
2.	0.00368713	0.000396623	0.0000327027

$$\begin{aligned}
 u_1(\varphi, t) &= \frac{t^\mu}{8\Gamma(1+\mu)} \cos(\varphi) \tanh(\varphi) (c1 \\
 &\quad + c2 \cos^2(\varphi) \tanh^2(\varphi)) \\
 &\quad \times (16 \cos(\varphi) \operatorname{sech}^2(\varphi) - 17 \sin(\varphi) \tanh(\varphi)) \\
 v_1(\varphi, t) &= \frac{t^\mu}{8\Gamma(1+\mu)} \sin^4(\varphi) \tanh^4(\varphi) (c3 \\
 &\quad + c4 \sin(\varphi) \tanh(\varphi)) \\
 &\quad \times (17 \cos(\varphi) \tanh(\varphi) + 16 \sin(\varphi) \operatorname{sech}^2(\varphi)) \\
 w_1(\varphi, t) &= -\frac{9t^\mu}{\Gamma(1+\mu)} \tanh(\varphi) \left( \frac{7}{8} - 2 \tanh^2(\varphi) \right)^6 \operatorname{sech}^2 \\
 &\quad (\varphi) \\
 &\quad \times \left( c5 - 2c6 \tanh^2(\varphi) + \frac{7c6}{8} \right).
 \end{aligned} \tag{21}$$

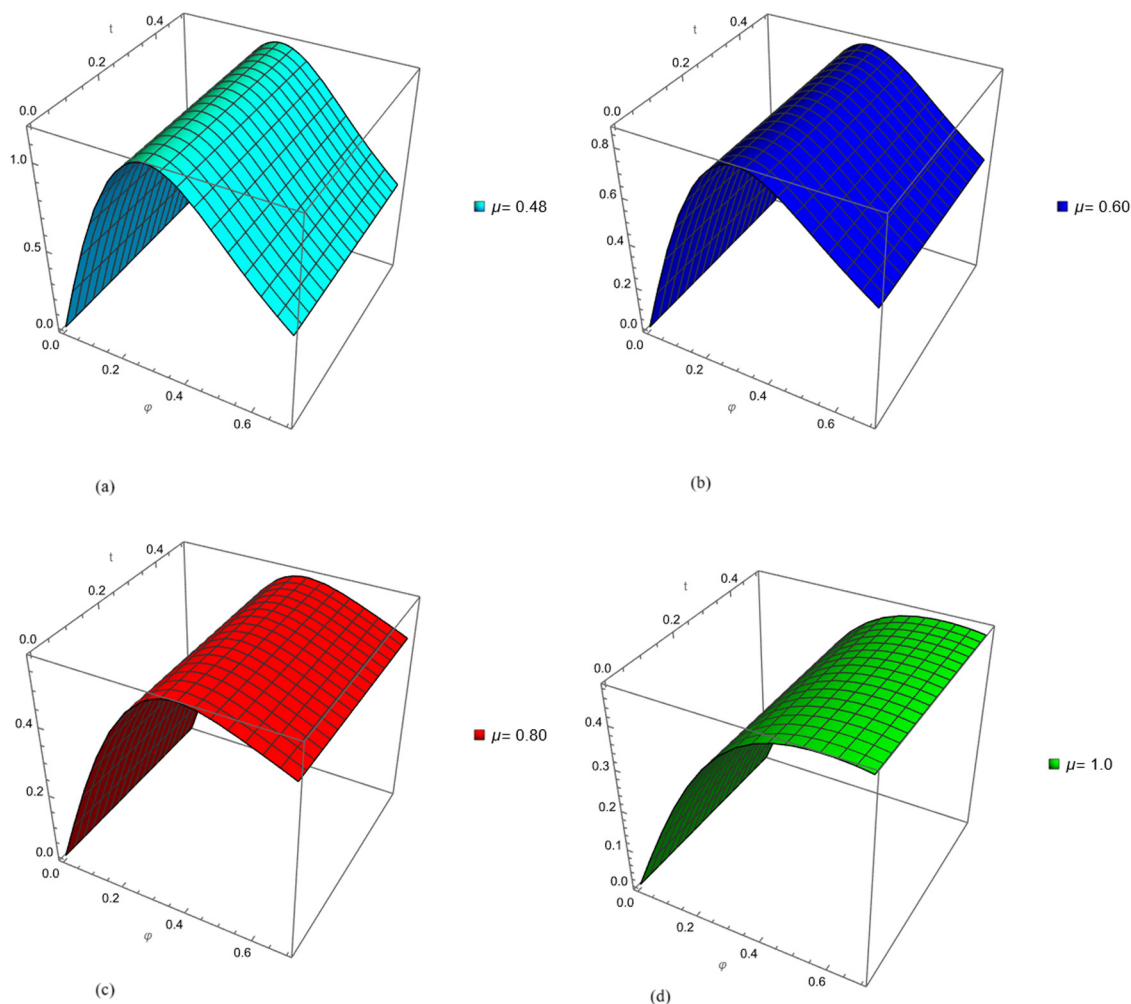


**Figure 1:** The fractional order of (a)  $\mu = 0.4$ , (b) OAFM  $\mu = 0.6$ , (c)  $\mu = 0.8$ , and (d)  $\mu = 1$  of  $u(\varphi, t)$  at  $t = 0.004$ .



According to the OAFM procedure,

$$\begin{aligned} u(\varphi, t) &= u_0(\varphi, t) + u_1(\varphi, t), \\ v(\varphi, t) &= v_0(\varphi, t) + v_1(\varphi, t), \\ w(\varphi, t) &= w_0(\varphi, t) + w_1(\varphi, t). \end{aligned} \quad (22)$$

Using Eqs (16) and (21), we have

$$\begin{aligned} u(\zeta, t) &= \cos(\varphi) \tanh(\varphi) + \frac{t^\mu}{8\Gamma(1+\mu)} \cos(\varphi) \tanh(\varphi) \\ &\quad \times (c_1 + c_2 \cos^2(\varphi) \tanh^2(\varphi)) \\ &\quad \times (16 \cos(\varphi) \operatorname{sech}^2(\varphi) - 17 \sin(\varphi) \tanh(\varphi)), \\ v(\zeta, t) &= \sin(\varphi) \tanh(\varphi) + \frac{t^\mu}{8\Gamma(1+\mu)} \sin^4(\varphi) \tanh^4(\varphi) \\ &\quad \times (c_3 + c_4 \sin(\varphi) \tanh(\varphi))(17 \cos(\varphi) \tanh(\varphi) \\ &\quad + 16 \sin(\varphi) \operatorname{sech}^2(\varphi)), \\ w(\zeta, t) &= \frac{7}{8} - 2 \tanh^2(\varphi) - \frac{9t^\mu}{\Gamma(1+\mu)} \tanh(\varphi) \\ &\quad \times \left( \frac{7}{8} - 2 \tanh^2(\varphi) \right)^6 \operatorname{sech}^2(\varphi) \\ &\quad \times \left[ c_5 - 2c_6 \tanh^2(\varphi) + \frac{7c_6}{8} \right]. \end{aligned} \quad (23)$$

The exact result is given as (Tables 1, 2, and 3).

## 4 Numerical and graphical results

The graphical analysis in this section provides insights into the behavior of the solutions to the nonlinear system of coupled Schrodinger–KdV equations with varying fractional orders ( $\mu$ ) at a specific time point ( $t = 0.004$ ). Figure 1 shows the set of graphs that depicts the behavior of the function  $u(\varphi, t)$  at  $t = 0.004$  for different fractional orders: (a)  $\mu = 0.4$ , (b)  $\mu = 0.6$ , (c)  $\mu = 0.8$ , and (d)  $\mu = 1$ . These visualizations illustrate how changing the fractional order affects the behavior of  $u$  at this specific time instance, shedding light on the impact of fractional order on the solution. Similarly, Figure 2 presents the behavior of the function  $v(\varphi, t)$  at  $t = 0.004$  for various fractional orders: (a)  $\mu = 0.6$ , (b)  $\mu = 0.7$ , (c)  $\mu = 0.8$ , and (d)  $\mu = 1$ . These graphs allow us to observe how altering the fractional order influences the characteristics of  $v$  at this particular time. Figure 3 focuses on the function  $w(\varphi, t)$  at  $t = 0.004$  under different

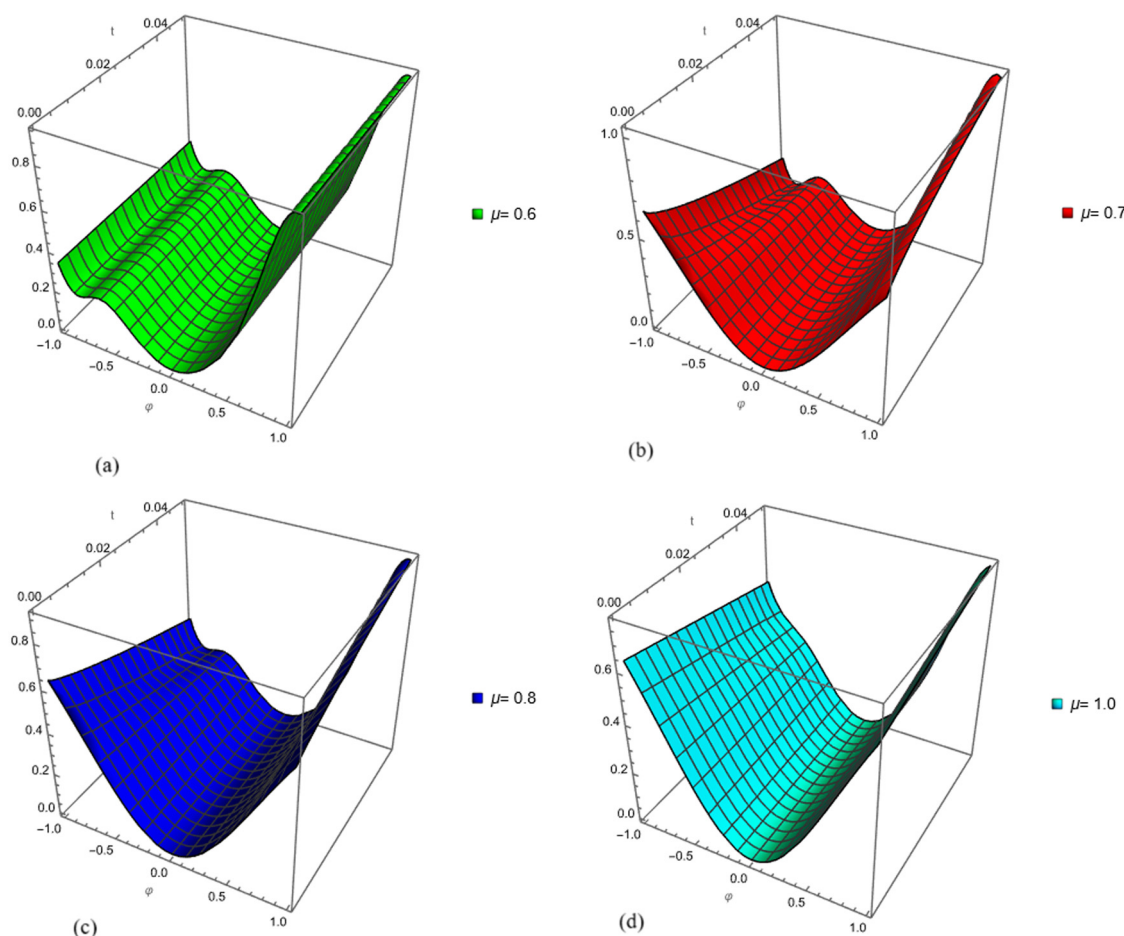


**Figure 2:** The fractional order of (a)  $\mu = 0.6$ , (b)  $\mu = 0.7$ , (c)  $\mu = 0.8$ , and (d)  $\mu = 1$  of  $v(\varphi, t)$  at  $t = 0.004$ .

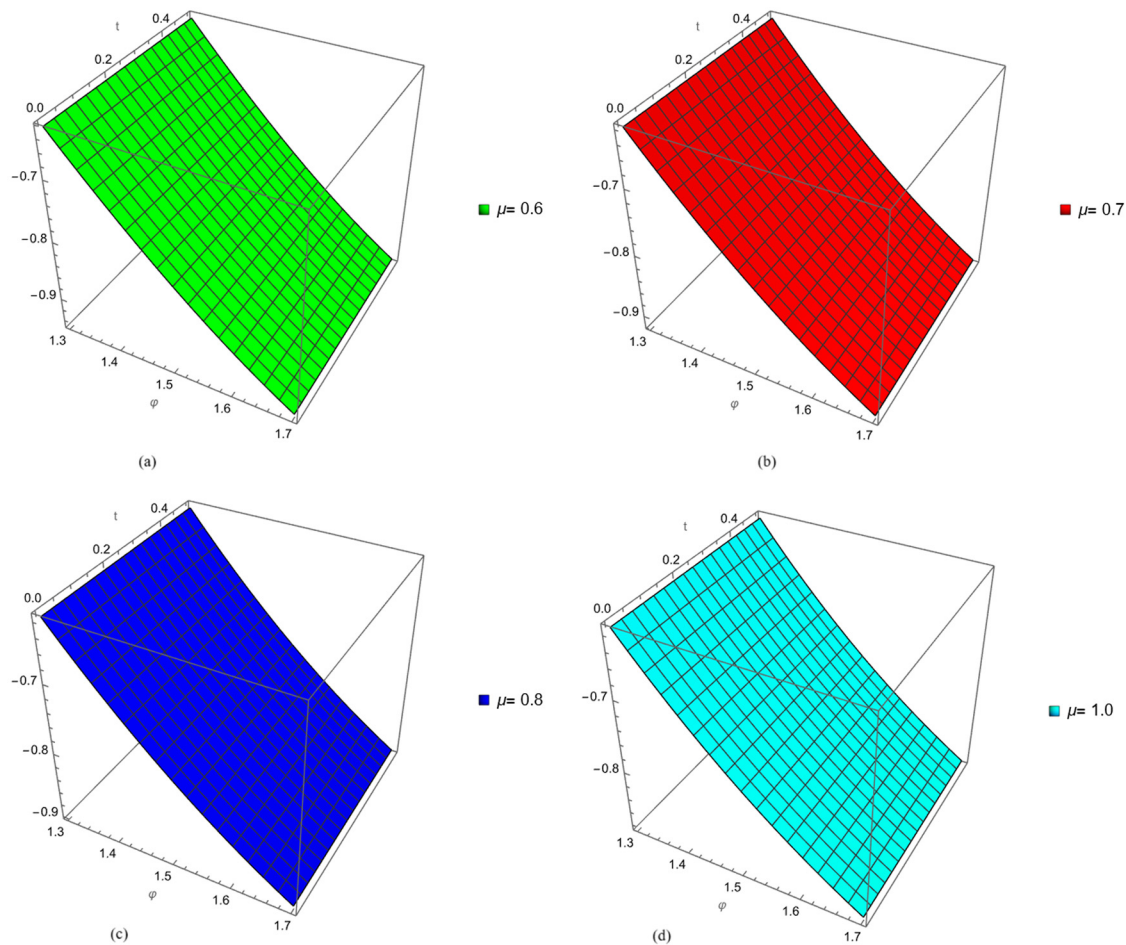


**Figure 3:** The fractional order of (a)  $\mu = 0.6$ , (b)  $\mu = 0.7$ , (c)  $\mu = 0.8$ , and (d)  $\mu = 1$  of  $w(\varphi, t)$  at  $t = 0.004$ .

fractional order conditions: (a)  $\mu = 0.6$ , (b)  $\mu = 0.7$ , (c)  $\mu = 0.8$ , and (d)  $\mu = 1$ . These visual representations enable us to explore the variations in the behavior of  $w$  as the fractional order  $\mu$  changes. By examining these figures, one can gain a better understanding of how the fractional order parameter ( $\mu$ ) influences the solutions  $u$ ,  $v$ , and  $w$  in the nonlinear system of coupled Schrödinger–KdV equations. These graphical representations provide valuable insights into the dynamics of the system at a specific time point and the role of the fractional order in shaping these dynamics.

## 5 Conclusion

Finally, this research ventured into the domain of nonlinear systems by using the OAFM to evaluate a coupled system of Schrödinger–KdV equations using the Caputo operator. The OAFM demonstrated its effectiveness in handling difficult nonlinear issues by approximating solutions to

the intricate dynamics of the coupled equations. The reported numerical and graphical assessments proved the method's correctness and efficiency, demonstrating its potential for dealing with difficult mathematical physics problems. This research adds to a greater knowledge of coupled Schrödinger–KdV equations and their ramifications across numerous scientific areas by effectively revealing insights into the behavior of the nonlinear system. The OAFM's relevance as a useful instrument in the arsenal of mathematical analysis is reinforced by its capacity to offer trustworthy solutions to complex nonlinear systems.

**Acknowledgments:** This work received support from the Princess Nourah bint Abdulrahman University Researchers Supporting Project number (PNURSP2023R183), Princess Nourah bint Abdulrahman University, Riyadh, Saudi Arabia. This work was supported by the Deanship of Scientific Research, the Vice Presidency for Graduate Studies and Scientific Research, King Faisal University, Saudi Arabia (Grant No. 4447).

**Funding information:** This work received support from the Princess Nourah bint Abdulrahman University Researchers Supporting Project number (PNURSP2023R183), Princess Nourah bint Abdulrahman University, Riyadh, Saudi Arabia. This work was supported by the Deanship of Scientific Research, the Vice Presidency for Graduate Studies and Scientific Research, King Faisal University, Saudi Arabia (Grant No. 4447).

**Author contributions:** All authors have accepted responsibility for the entire content of this manuscript and approved its submission.

**Conflict of interest:** The authors state no conflict of interest.

## References

- [1] Deepika S, Veeresha P. Dynamics of chaotic waterwheel model with the asymmetric flow within the frame of Caputo fractional operator. *Chaos Solitons Fractals*. 2023;169:113298.
- [2] Premakumari RN, Baishya C, Veeresha P, Akinyemi L. A fractional atmospheric circulation system under the influence of a sliding mode controller. *Symmetry*. 2022;14(12):2618.
- [3] Ilhan E, Veeresha P, Baskonus HM. Fractional approach for a mathematical model of atmospheric dynamics of CO<sub>2</sub> gas with an efficient method. *Chaos Solitons Fractals*. 2021;152:111347.
- [4] Gao W, Veeresha P, Cattani C, Baishya C, Baskonus HM. Modified predictor-corrector method for the numerical solution of a fractional-order SIR model with 2019-nCoV. *Fractal and Fractional*. 2022;6(2):92.
- [5] Akinyemi L, Veeresha P, Ajibola SO. Numerical simulation for coupled nonlinear Schrödinger-Korteweg-de Vries and Maccari systems of equations. *Modern Phys Lett B*. 2021;35(20):2150339.
- [6] Veeresha P, Ilhan E, Baskonus HM. Fractional approach for analysis of the model describing wind-influenced projectile motion. *Physica Scripta*. 2021;96(7):075209.
- [7] Alderremy AA, Aly S, Fayyaz R, Khan A, Wyal N. The analysis of fractional-order nonlinear systems of third order KdV and Burgers equations via a novel transform. *Complexity*. 2022;2022:4935809.
- [8] Fu H, Wang H, Wang Z. POD/DEIM reduced-order modeling of time-fractional partial differential equations with applications in parameter identification. *J Scientif Comput*. 2018;74:220–43.
- [9] Sunthrayuth P, Aljahdaly NH, Ali A, Mahariq I, Tchalla AM. psi-Haar wavelet operational matrix method for fractional relaxation-oscillation equations containing  $\psi$ -Caputo fractional derivative. *J Funct Spaces*. 2021;2021:1–14.
- [10] Yasmin H, Aljahdaly NH, Saeed AM. Probing families of optical soliton solutions in fractional perturbed Radhakrishnan-Kundu-Lakshmanan model with improved versions of extended direct algebraic method. *Fractal Fraction* 2023;7(7):512.
- [11] Yasmin H, Alshehry AS, Khan A, Nonlaopon K. Numerical analysis of the fractional-order Belousov-Zhabotinsky system. *Symmetry*. 2023;15(4):834.
- [12] Veeresha P. The efficient fractional order based approach to analyze chemical reaction associated with pattern formation. *Chaos Solitons Fractals*. 2022;165:112862.
- [13] Song J, Mingotti A, Zhang J, Peretto L, Wen H. Accurate damping factor and frequency estimation for damped real-valued sinusoidal signals. *IEEE Trans Instrument Measurement*. 2022;71:6503504. doi: 10.1109/TIM.2022.3220300.
- [14] Hu D, Li Y, Yang X, Liang X, Zhang K, Liang X, et al. Experiment and application of NATM tunnel deformation monitoring based on 3D laser scanning. *Struct Control Health Monitor*. 2023;2023:3341788. doi: 10.1155/2023/3341788.
- [15] Guo C, Hu J, Hao J, Celikovsky S, Hu X. Fixed-time safe tracking control of uncertain high-order nonlinear pure-feedback systems via unified transformation functions. *Kybernetika*. 2023;59(3):342–64. doi: 10.14736/kyb-2023-3-0342.
- [16] Yasmin H, Aljahdaly NH, Saeed AM, Shah R. Probing families of optical soliton solutions in fractional perturbed Radhakrishnan-Kundu-Lakshmanan model with improved versions of extended direct algebraic method. *Fractal Fractional*. 2023;7(7):512.
- [17] Yasmin H, Aljahdaly NH, Saeed AM. Investigating families of soliton solutions for the complex structured coupled fractional Biswas-Arshed model in birefringent fibers using a novel analytical technique. *Fractal Fractional*. 2023;7(7):491.
- [18] Yasmin H, Aljahdaly NH, Saeed AM, Shah R. Investigating symmetric soliton solutions for the fractional coupled Konno-Onno system using improved versions of a novel analytical technique. *Mathematics*. 2023;11(12):2686.
- [19] Shafee A, Alkhezi Y. Efficient solution of fractional system partial differential equations using Laplace residual power series method. *Fractal Fract*. 2023;7(6):429.
- [20] Mason LJ, Sparling GA. Nonlinear Schrödinger and Korteweg-de Vries are reductions of self-dual Yang-Mills. *Phys Lett A*. 1989;137(1–2):29–33.
- [21] Klein C. Fourth order time-stepping for low dispersion Korteweg-de Vries and nonlinear Schrödinger equation. *Electron Trans Numer Anal*. 2008;29(116–135):37.
- [22] Noor S, Alotaibi BM, Ismaeel SM, El-Tantawy SA. On the solitary waves and nonlinear oscillations to the fractional Schrödinger-KdV equation in the framework of the Caputo operator. *Symmetry*. 2023;15(8):1616.
- [23] Alshammari S, Al-Sawalha MM. Approximate analytical methods for a fractional-order nonlinear system of Jaulent-Miodek equation with energy-dependent Schrödinger potential. *Fractal Fract*. 2023;7(2):140.
- [24] Shah R, Hyder AA, Iqbal N, Botmart T. Fractional view evaluation system of Schrödinger-KdV equation by a comparative analysis. *AIMS Math*. 2022;7(11):19846–64.
- [25] Bekiranov D, Ogawa T, Ponce G. Weak solvability and well-posedness of a coupled Schrödinger-Korteweg de Vries equation for capillary-gravity wave interactions. *Proc Amer Math Soc*. 1997;125(10):2907–19.
- [26] Guo C, Hu J, Wu Y, Celikovsky S. Non-singular fixed-time tracking control of uncertain nonlinear pure-feedback systems with practical state constraints. *IEEE Trans Circuits Syst I Regular Papers*. 2023;70(9):3746–58. doi: 10.1109/TCSI.2023.3291700.
- [27] Meng Q, Ma Q, Shi Y. Adaptive fixed-time stabilization for a class of uncertain nonlinear systems. *IEEE Trans Automatic Control*. 2023. doi: 10.1109/TAC.2023.3244151.
- [28] Ma Q, Meng Q, Xu S. Distributed optimization for uncertain high-order nonlinear multiagent systems via dynamic gain approach.



- IEEE Trans Syst Man Cybernetics Syst. 2023;53(7):4351–7. doi: 10.1109/TSMC.2023.3247456.
- [29] Colorado E. On the existence of bound and ground states for some coupled nonlinear Schrödinger–Korteweg–de Vries equations. *Adv Nonlinear Anal.* 2017;6(4):407–26.
- [30] Song M, Qian X, Zhang H, Song S. Hamiltonian boundary value method for the nonlinear Schrödinger equation and the Korteweg–de Vries equation. *Adv Appl Math Mechanics.* 2017;9(4):868–86.
- [31] Liu Q, Peng H, Wang Z. Convergence to nonlinear diffusion waves for a hyperbolic-parabolic chemotaxis system modelling vasculogenesis. *J Differ Equ.* 2022;314:251–86. doi: <https://doi.org/10.1016/j.jde.2022.01.021>.
- [32] Jin H, Wang Z, Wu L. Global dynamics of a three-species spatial food chain model. *J Differ Equ.* 2022;333:144–83. doi: <https://doi.org/10.1016/j.jde.2022.06.007>.
- [33] Wang B, Shen Y, Li N, Zhang Y, Gao Z. An adaptive sliding mode fault-tolerant control of a quadrotor unmanned aerial vehicle with actuator faults and model uncertainties. *Int J Robust Nonlinear Control.* 2023. <https://doi.org/10.1002/rnc.6631>.
- [34] Wang B, Zhang Y, Zhang W. A composite adaptive fault-tolerant attitude control for a quadrotor UAV with multiple uncertainties. *J Syst Sci Complexity.* 2022;35(1):81–104. doi: 10.1007/s11424-022-1030-y.
- [35] Li Q, Lin H, Tan X, Du S.  $H^\infty$  consensus for multiagent-based supply chain systems under switching topology and uncertain demands. *IEEE Trans Syst Man Cybernetics Syst.* 2020;50(12):4905–18. doi: <https://doi.org/10.1109/TSMC.2018.2884510>.
- [36] Zhang X, Lu Z, Yuan X, Wang Y, Shen X. L2-gain adaptive robust control for hybrid energy storage system in electric vehicles. *IEEE Trans Power Electron.* 2021;36(6):7319–32. doi: <https://doi.org/10.1109/TPEL.2020.3041653>.
- [37] Taghieh A, Zhang C, Alattas KA, Bouteraa Y, Rathinasamy S, Mohammadzadeh A. A predictive type-3 fuzzy control for under-actuated surface vehicles. *Ocean Eng.* 2022;266:113014. doi: <https://doi.org/10.1016/j.oceaneng.2022.113014>.
- [38] Bai X, He Y, Xu M. Low-thrust reconfiguration strategy and optimization for formation flying using Jordan normal form. *IEEE Trans Aerospace Electronic Syst.* 2021;57(5):3279–95. doi: <https://doi.org/10.1109/TAES.2021.3074204>.
- [39] Sun W, Wang H, Qu R. A novel data generation and quantitative characterization method of motor static eccentricity with adversarial network. *IEEE Trans Power Electronics.* 2023;38(7):8027–32. doi: <https://doi.org/10.1109/TPEL.2023.3267883>.
- [40] Lu S, Ding Y, Liu M, Yin Z, Yin L, Zheng W. Multiscale feature extraction and fusion of image and text in VQA. *Int J Comput Intell Syst.* 2020;16(1):54. doi: <https://doi.org/10.1007/s44196-023-00233-6>.
- [41] Yin L, Wang L, Li T, Lu S, Yin Z, Liu X, et al. U-Net-STN: A novel end-to-end lake boundary prediction model. *Land.* 2023;12(8):1602. doi: 10.3390/land12081602.
- [42] Chen D, Wang Q, Li Y, Li Y, Zhou H, Fan Y. A general linear free energy relationship for predicting partition coefficients of neutral organic compounds. *Chemosphere.* 2020;247:125869. doi: 10.1016/j.chemosphere.2020.125869.
- [43] Lu S, Liu M, Yin L, Yin Z, Liu X, Zheng W, et al. The multi-modal fusion in visual question answering: a review of attention mechanisms. *Peer J Comput Sci.* 2023;9:e1400. doi: 10.7717/peerjcs.1400.